

## INFLUENCE STEEL MANUFACTURING PROCESS **X2CrNiMoN25-7-4 ON ITS STRUCTURE**

**Paweł Szabracki<sup>1</sup>, Tomasz Lipiński<sup>1</sup>, Miroslaw Bramowicz<sup>1</sup>,**  
**Kazimierz Rychlik<sup>2</sup>**

<sup>1</sup> Chair of Materials and Machinery Technology  
University of Warmia and Mazury in Olsztyn

<sup>2</sup> Department of Mechanised Construction  
Institute of Mechanised Construction and Rock Mining

**K e y w o r d s:** X-Ray diffraction, XRD, duplex steel.

### A b s t r a c t

This paper presents results of X2CrNiMoN25-7-4 steel structure investigation. Measurements were carried out in commercial state and after additional solution heat treatment. The structure analysis was carried out based on XRD measurements. Obtained results allowed for determination of structure parameters, phase's volume and lattice defects.

Obtained results suggested, that applied finishing treatments didn't influent on structure parameters and the lattice defects.

### WPŁYW PROCESU WYTWARZANIA STALI X2CrNiMoN25-7-4 NA JEJ BUDOWĘ STRUKTURALNĄ

**Paweł Szabracki<sup>1</sup>, Tomasz Lipiński<sup>1</sup>, Miroslaw Bramowicz<sup>1</sup>, Kazimierz Rychlik<sup>2</sup>**

<sup>1</sup> Katedra Technologii Materiałów i Maszyn  
Uniwersytet Warmińsko-Mazurski w Olsztynie

<sup>2</sup> Zakład Obrabiarek i Technologii Montażu  
Instytut Mechanizacji Budownictwa i Górnictwa Skalnego

**S l o w a k l u c z o w e:** dyfraktometria rentgenowska, XRD, stal dupleks.

### A b s t r a c t

W pracy przedstawiono wyniki badań struktury stali X2CrNiMoN25-7-4. Badania przeprowadzono dla stanu komercyjnego materiału oraz po procesie powtórnego przesycania. Strukturę materiału analizowano na podstawie pomiarów dyfraktometrycznych. Określono parametry sieciowe składników, stopień zdefektowania struktury oraz wyznaczono udziały fazowe. Analiza wyników badań wykazała, że stosowane na etapie produkcji zabiegi wykańczające nie wpłynęły na parametry strukturalne oraz stopień zdefektowania struktury.

## Introduction

Properties of chrome-nickel in austenitic-ferritic structure combines advantages and elimination (or substantial minimization) defects of single-phase (ferrite, austenite) stainless steels. Main advantages of this type of material are: high yield and tensile strength and high resistance to stress corrosion and pitting corrosion. These properties make this type of steel, very attractive construction material, mainly in industry: chemical, petrochemical, mining and shipbuilding. They are produced, among others through properly maintained phase proportions of shares in structure of material. In this type of stainless steels ferrite volume fraction is between 40–60%, but optimum mechanical properties and corrosion resistance is achieved with a 50% volume fraction of austenite and ferrite (LEE et al. 2002, LIPIŃSKI et al. 2010). Increase volume fraction of ferrite in stainless steel structure increases yield strength, tensile strength and hardness, while reducing corrosion resistance of material and ductility and toughness. It is particularly important to maintain appropriate phase volume fraction in welded joints in order to ensure performance of material.

During welding processes, as well as during heat treatment in temperature range from 300–1000°C in austenite and ferrite can nucleate and grow vary in terms of chemical composition and structure phases, for example, secondary austenite, many carbides and nitrides, sigma phase  $\sigma$ , or causing so-called. 475°C fragility rich in chromium ferrite $\alpha'$  (NOWACKI 2008, LAI et al. 1995). Presence of 1–2% in structure of sigma phase  $\sigma$ , may reduce toughness of steel by half, and with participation of this phase, more than 5% following a sharp drop in corrosion resistance and almost disappearance of plasticity (LIPIŃSKI 1993, LIPSON 2001).

These steels are produced by continuous casting followed by giving dimensions of material in hot rolling process. After rolling process is used solutioning. In some technologies, last step of production process is also used in cold rolling, as a finishing treatment. Depending on degree of deformation it can introduce stress and plastic deformation.

Production technologies are property of steel mills, and are not made available to their customers.

Through comparative researches, commercial material with material known treated technology, it can be concluded about state of material available commercially.

## Aim and methodology of research

Aim of this study was to analyze impact of steel-making process on its structure.

Subject of research in this study were samples of steel X2CrNiMoN25-7-4, taken from cold-rolled sheet of steel.

Due to texture present in rolled materials, in order to consideration of a privileged orientation of crystallites on intensity of diffraction reflexes in carried out calculations taken into account all recorded diffraction reflexes.

To achieve objective of study decided to compare structural parameters of selected steel in a commercial state with steel saturated from temperature 1100°C. Austenitizing time taken for 30 minutes.

Using X-ray diffraction research (XRD) determined lattice parameters of structural components, degree of lattice defects and calculated phase volume fraction.

## X-ray diffraction research (XRD)

XRD studies were carried out on X-ray diffractometer XPERT PRO with focusing rays by Bragg-Brentano and registration stepping pulses. Measurements were made in range of 2θ angles from 30–120° using CuK $\alpha$  radiation and pulse counting time at each angular position, equal to 2 seconds.

Based on recorded diffraction patterns of tested stainless steel determined lattice parameters of ferrite and austenite, determined phases volume fraction of present phases and determined size of coherently scattering regions of X-rays (mosaic blocks) and distortion of lattice, reflecting degree of defects in phase structure of individual components.

Contained in diffraction patterns data describing structure and material properties are associated with location and size of diffraction peaks, so to accurately determine angular positions of individual reflexes and to designate areas contained between curve describing profile of peak and background line was used Winfit program.

Applied program also enabled numerical correction half-width (FWHM) and intensity coming from component of K $\alpha$ 2 X-ray. Profile shape of each reflexes described with Cauchy function, according to which intensity of deflected beam of X-rays are described by formula (1) (SENCZYK 1996).

$$I(\Theta) = I_0 \frac{1}{1 + kx^2} \quad (1)$$

where:

- $I_0$  – intensity of incident beam,
- $k$  – function parameter (determined by least square method),
- $x$  – scaled value of angle  $\theta$ .

Shape and position of reflexes are related to physical factors which characterize a given structure, such as: microstresses, size of mosaic blocks, lattice distortion, and instrumental factors. Width of reflexes are defined as so-called integral width expressed as ratio of area contained between curve describing profile of peak and background line to maximum intensity, or as a half-width (FWHM) reflexes (CULLITY 1964). Physical width of diffraction reflexes  $\beta$  is sum of three components: instrumental ( $\beta_i$ ), coming from lattice distortion ( $\beta_z$ ) and component related to size of crystallites ( $\beta_k$ ) (BOJARSKI, BOŁD 1970, BOJARSKI, ŁĄGIEWKA 1988, CULLITY 1964).

In order to eliminate instrumental broadening, having a significant impact on half-width (FWHM) and integral intensity, thus to set size of blocks and distortions in lattice, performed using standard diffraction pattern of polycrystalline silicon, under same diffractometer operating parameters and conditions as measurement tested samples of stainless steel.

Diffraction pattern of polycrystalline silicon and influence of factors on apparatus half-width of registered reflexes as a function of angle  $2\theta$  are shown in Figure 1. For measurement conditions, change width FWHM describes determined formula (2).

$$y(2\theta) = 0,072 + 2\theta \cdot 1,418 \cdot 10^{-3} - (2\theta)^2 \cdot 1,99 \cdot 10^{-5} + (2\theta)^3 \cdot 1,207 \cdot 10^{-7} \quad (2)$$

Formula (2) allows to determine real reflexes width ( $\beta_r$ ) which for profiles described with Cauchy function is:  $\beta_r = \beta - \beta_i$  (BOJARSKI, ŁĄGIEWKA 1988).

### Methodology for determining lattice parameters and phase volume fractions

To determine lattice parameters of ferrite ( $\alpha$ ) and austenite ( $\gamma$ ) used linear extrapolation of lattice parameters determined on basis of angular positions of peaks coming from various phases:  $\alpha$  and  $\gamma$  and angle of reflection  $\Theta = 90^\circ$ . As a function of extrapolation was used as described by formula (3) function Nelson-Riley (N-R) (LIPSON 2001).

$$f(\Theta) = \frac{1}{2} \left( \frac{\cos^2(\Theta)}{\sin(\Theta)} + \frac{\cos^2(\Theta)}{\Theta} \right) \quad (3)$$

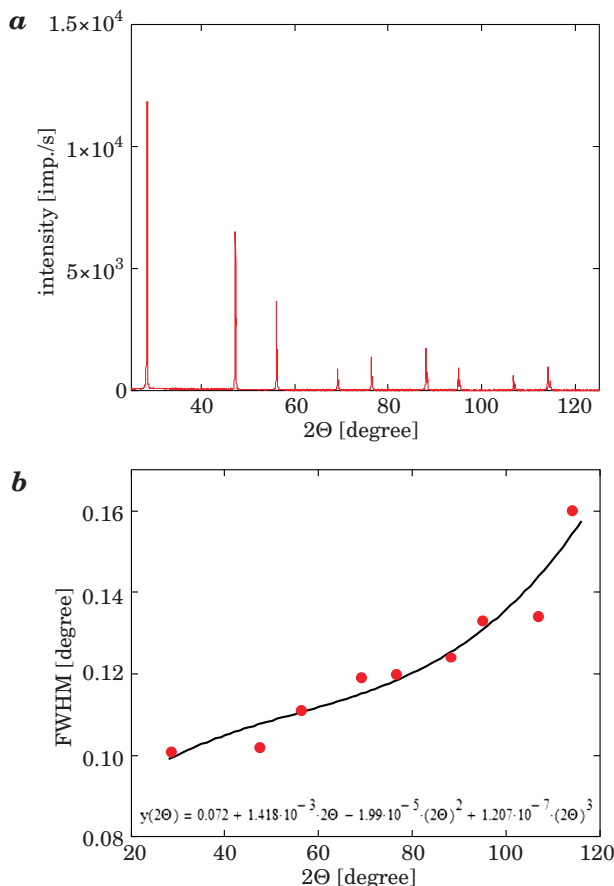


Fig. 1. Diffraction pattern (a) standard of polycrystalline silicon, and relationship (b) showing the diffractometer instrumental broadening, for the measurement conditions

Determination of phase volume fraction by X-ray phase analysis method based on principle, according to which intensity of diffraction peaks depend on fraction of various phases (BOJARSKI, ŁAGIEWKA 1988, CULLITY 1964).

In case of material with privileged orientation, intensity of reflex coming from each phase describes relationship (4) (BOJARSKI, ŁAGIEWKA 1988):

$$J_{hkl}^j = K_j \frac{m_j}{\mu} P_{hkl} \quad (4)$$

where:

- $m_j$  – mass fraction of phase  $j$  in mixture,
- $\mu$  – mass absorption coefficient of mixture,

- $P_{hkl}$  – ratio of crystallites are in position satisfying Bragg condition, for planes  $(hkl)$ ,
- $K'$  – value described by formula (5) – dependent on constant geometrical conditions (eg. diffractometer radius, cross-sectional area of original beam) during performing diffraction patterns and crystalline structure.

$$K'_j = C \cdot \frac{1}{\nu^2} \cdot |F_{hkl}|^2 \cdot LP \cdot p \cdot e^{-2M} \quad (5)$$

$|F_{hkl}|^2$  – square structure factor, whose value for austenite and ferrite is respectively:  $16f_{sr}^2$  i  $4f_{sr}^2$ , where  $f_{sr}$  is average atomic scattering factor for alloy. Average atomic scattering factor take into account chemical composition of tested steel and atomic fraction of individual elements. Value of this factor for tested material describe formula (6):

$$f_{sr} = 0,62f_{Fe} + 0,27f_{Cr} + 0,06f_{Ni} + 0,02f_{Mo} + 0,01f_N + (4,53f_{Si} + 7,85f_{Mn} + 2f_{Cu} + 1,13f_{Co}) \cdot 10^{-3} + (7,83f_C + 3,93f_P \cdot 10^{-4} + (1,72f_S + 8,33f_{Nb}) \cdot 10^{-5}) \quad (6)$$

Values of each atomic factors derived from constituent elements read relation  $f_i = f \left( \frac{\sin \theta}{\lambda} \right)$  ( $i$  – symbol element), using for this purpose a computer program *Krystalografia2* described in paper (BOJARSKI 1988).

LP – Lorenz–Thomson factor, equal:  $\frac{1 + \cos^2(1\Theta)}{\sin^2 \Theta \cos \Theta} - \frac{1 + \cos^2(\Theta)}{\sin^2 \Theta \cos \Theta}$

$p$  – factor times diffraction planes – determined on basis of tables contained in (CULLITY 1964),

$e^{-2M}$  – temperature coefficient.

Considering above equations, fraction of m-phase in mixture of  $\alpha$  and  $\gamma$  can be described as (7):

$$m_{\alpha, \gamma} = \frac{\frac{1}{n} \sum_{i=1}^n \frac{J'_{ihkl}}{K'_{i\alpha\gamma}}}{\frac{1}{n} \sum_{i=1}^n \frac{J'_{ihkl}}{K'_{i\alpha\gamma}} + \frac{1}{k} \sum_{i=1}^k \frac{J'_{ihkl}}{K'_{i\alpha\gamma}}} \quad (7)$$

where:  $n$  and  $k$  are respectively number of peaks coming respectively from phase  $\alpha$  and  $\gamma$ .

Values of basic parameters necessary to carry out phase analysis and results are summarized in tables: 1 and 2.

Factor characterizing structural construction occurring phases can be also size of areas coherently scattering X-rays (mosaic blocks) and a occurring distortion of lattice (BOJARSKI, BOŁD 1970).

In order to determine those parameters was used by Williamson-Hall method (W-H) (BOJARSKI, ŁĄGIEWKA 1988). According to this method, for peak profiles described Cauchy function, total actual diffraction line broadening ( $\beta_r$ ) is sum of extensions coming from size of blocks ( $\beta_k$ ) and distortion of lattice ( $\beta_z$ ), so:

$$\beta_r = \beta_k + \beta_z \quad (8)$$

$\beta_k$  component is described by Scherrer relationship (8) (BOJARSKI, ŁĄGIEWKA 1988, CULLITY 1964):

$$\beta_k = \frac{K\lambda}{D_{hkl} \cos\Theta} \quad (9)$$

where:

$K$  – Scherrer constant,

$\lambda$  – X-ray wavelength,

$D_{hkl}$  – average crystallite size (blocks) in a direction perpendicular to planes ( $hkl$ ),

$\Theta$  – reflection angle,

$hkl$  – Miller indices.

However  $\beta_z$  component of distortion resulting from lattice describes Taylor's relationship (10) (BOJARSKI, ŁĄGIEWKA 1988):

$$\beta_z = 4 \left( \frac{\Delta a}{a} \right) \operatorname{tg}\theta \quad (10)$$

Taking into account dependence (9) and (10) equation for total actual broadening of diffraction peak becomes a (11) (BOJARSKI, ŁĄGIEWKA 1988):

$$\beta_r \cos\theta = \frac{K\lambda}{D} + 4 \left( \frac{\Delta a}{a} \right) \sin\theta \quad (11)$$

By linear regression plotting relationship  $\beta \cdot \cos \theta = f(\sin \theta)$  for several reflexes of same sample (best for several rows of reflections from same plane ( $hkl$ )) ordinate values can be determined crystallite size (mosaic blocks), while value of slope to determine distortion of lattice (stresses of second kind). Defined and further described X-ray parameters used in testing methods based on X-ray diffraction on crystal lattice can be found in papers (BOJARSKI, ŁAGIEWKA 1988, CULLITY 1964).

## Research results and their analysis

Recorded during measurements of X-ray diffraction patterns (Fig. 2) and associated interdependence of reflection angles of particular diffraction reflexes clearly indicate presence of two structural components of regular lattice: ferrite ( $\alpha$ ) – with symmetry  $I\frac{4}{m}\bar{3}\frac{2}{m}$  (space group 229) and austenite ( $\gamma$ ) – with symmetry  $F\frac{4}{m}\bar{3}\frac{2}{m}$  (space group 225).

Plotting relationship lattice parameters  $a_{hkl}$ , determined on basis of angular positions Bragg each reflexes, depending on value function N-R (described

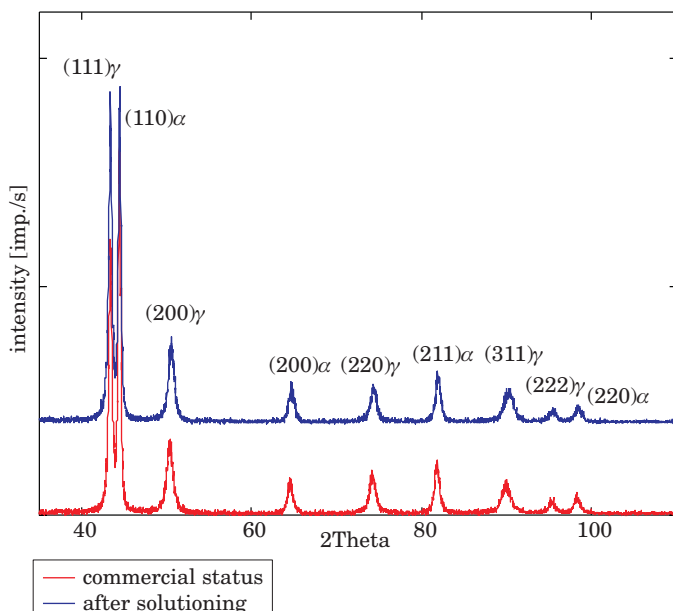


Fig. 2. Diffraction pattern of stainless steel X2CrNiMoN25-7-4: commercial status and after solutioning

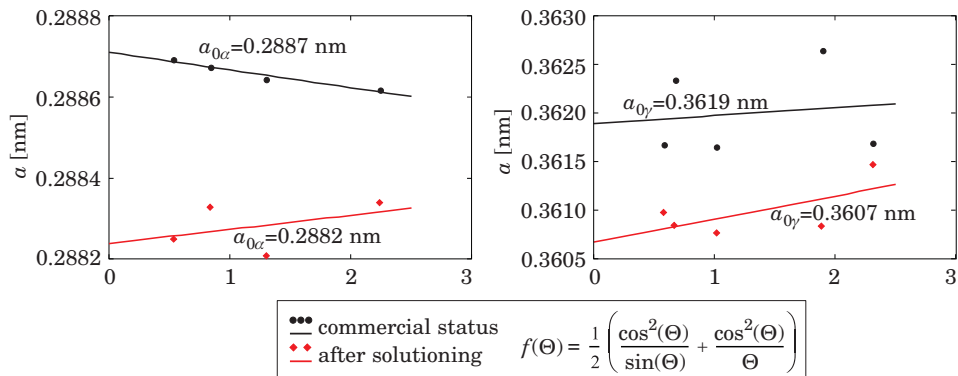
by formula 3) and made linear extrapolation function N-R to a value corresponding to reflection angle  $\theta$  equal 90 degree. Determined by method of extrapolation of lattice parameters of ferrite and austenite,  $a_0$  are respectively: for commercial status 2.887 Å and 3.619 Å and after solutioning 2.882 Å and

Table 1  
Summary of main parameters and XRD results for samples of stainless steel X2CrNiMoN25-7-4 in commercial status

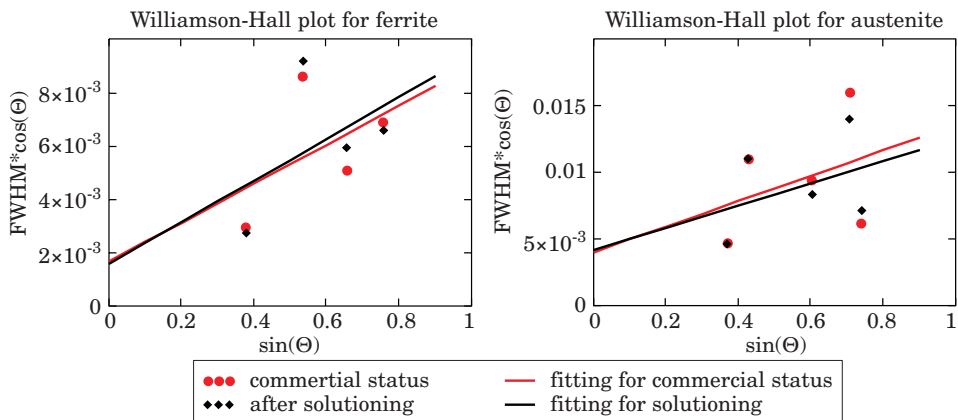
Ferrite									
No.	<i>hkl</i>	2Θ	<i>I</i>	$f_{sr}$	<i>p</i>	LP	$ F_{hkl} ^2$	$a_{0(\alpha)}$ [Å]	$V_\alpha$ [%]
1.	110	44.351	233	17.93	12	11.46	1285.4	2.887	46.72
2.	200	64.517	56	15.13	6	4.92	915.75		
3.	211	81.631	69	13.33	24	3.16	710.30		
4.	220	97.997	27	12.11	12	2.73	587.10		
Austenite									
No.	<i>hkl</i>	2Θ	<i>I</i>	$f_{sr}$	<i>p</i>	LP	$ F_{hkl} ^2$	$a_{0(\gamma)}$ [Å]	$V_\gamma$ [%]
1.	111	43.293	239	18.10	8	12.10	5244.1	3.619	53.28
2.	200	50.28	117	17.03	6	8.62	4642.1		
3.	220	74.09	57	14.04	12	3.71	3155.0		
4.	311	89.674	93	12.69	24	2.84	2575.0		
5.	222	95.088	18	12.31	8	2.74	2423.6		

Table 2  
Summary of main parameters and XRD results for samples of stainless steel X2CrNiMoN25-7-4 after solutioning

Ferrite									
No.	<i>hkl</i>	2Θ	<i>I</i>	$f_{sr}$	<i>p</i>	LP	$ F_{hkl} ^2$	$a_{0(\alpha)}$ [Å]	$V_\alpha$ [%]
1.	110	44.396	219	17.93	12	11.43	1285.4	2.882	44.91
2.	200	64.626	59	15.13	6	4.90	915.7		
3.	211	81.75	63	13.33	24	3.15	710.3		
4.	220	98.20	23	12.11	12	2.73	587.1		
Austenite									
No.	<i>hkl</i>	2Θ	<i>I</i>	$f_{sr}$	<i>p</i>	LP	$ F_{hkl} ^2$	$a_{0(\gamma)}$ [Å]	$V_\gamma$ [%]
1.	111	43.321	283	18.10	8	12.08	5244.1	3.607	55.09
2.	200	50.549	148	17.03	6	8.52	4642.1		
3.	220	74.303	56	14.04	12	3.70	3155		
4.	311	90.147	62	12.69	24	2.82	2575		
5.	222	95.33	20	12.31	8	2.74	2423.6		

Fig. 3. Extrapolation of obtained lattice parameters:  $a$  – ferrite and  $b$  – austeniteTable 3  
Summary of size of mosaic blocks ( $D$ ) and distortion lattice  $\left\langle \frac{\Delta a}{a} \right\rangle$ 

Commercial status				Solutioning			
Ferrite		Austenite		Ferrite		Austenite	
$D$	$\left\langle \frac{\Delta a}{a} \right\rangle$	$D$	$\left\langle \frac{\Delta a}{a} \right\rangle$	$D$	$\left\langle \frac{\Delta a}{a} \right\rangle$	$D$	$\left\langle \frac{\Delta a}{a} \right\rangle$
[Å]	[%]	[Å]	[%]	[Å]	[%]	[Å]	[%]
836	0.18	346	0.24	880	0.19	331	0.21

Fig. 4. Williamson-Hall plots for:  $a$  – ferrite,  $b$  – austenite

3.607 Å. Dependencies  $a_{hkl} = f(N-R)$  shown in Figure 3. While detailed results of X-ray measurements and values of parameters necessary to carry out phase analysis are summarized in: table 1 and table 2.

Performed X-ray phase analysis of stainless steel samples X2CrNiMoN25-7-4 in commercial status and after solutioning gives similar results, both as to phase volume fraction and lattice parameters.

Also summarized in Table 3 size of mosaic blocks and distortions lattice derived from prepared Williamson-Hall plots (Fig. 4), show a similar degree of defects in crystal structure.

## Conclusion

Obtained lattice parameters for austenite and ferrite in commercial alloy and after solutioning are similar, as well as other parameters analyzed.

Analysis of results allowed to determine:

- commercial stainless steel is shipped as solutioning,
- technological process of steel production in industrial conditions provide for its two-phase structure,
- used in production stage finishing treatments did not affect its structural parameters.

Translated by AUTORS

Accepted for print 7.09.2011

## References

- BOJARSKI Z., GILA M., STRÓZ K., SUROWIEC M. 2001. *Krystalografia. Podręcznik wspomagany komputerowo*. PWN Warszawa.
- BOJARSKI Z., BOŁD T. 1970. *Rentgenograficzne metody wyznaczania zniekształceń sieciowych i wielkości bloków metali polikrystalicznych*. Prace Instytutów Hutniczych, 22.
- BOJARSKI Z., ŁĄGIEWKA E. 1988. *Rentgenowska analiza strukturalna*. Państwowe Wydawnictwo Naukowe, Warszawa.
- CULLITY B.D. 1964. *Podstawy dyfrakcji promieni rentgenowskich*. Państwowe Wydawnictwo Naukowe, Warszawa.
- LAI J.K.L., WONG K.W., LI D.J. 1995. *Effect of solution treatment on the transformation behaviour of cold-rolled duplex stainless steels*. Materials Science and Engineering, A203: 356–364.
- LEE S.C., KIM Y.H., LEE Y.D. 2002. *Analysis of creep deformation of type 2205 duplex stainless steel under continuous annealing conditions*. Journal of Materials Processing Technology, 123: 185–189.
- LIPIŃSKI T. 1993. *Analiza przyczyn pękania stali 1H18N9T podczas walcowania*. Mechanika. Tom III. Wyższa Szkoła Inżynierska w Zielonej Górze. Zielona Góra, pp. 41–44.
- LIPIŃSKI T., SZABRACKI P., BRAMOWICZ M., RYCHLIK K. 2010. *Computer modelling Structural components of Duplex stainless steel*. Process innovation, Charper 5, Dniepropetrovsk, pp. 56–69.
- LIPSON H. 2001. *The study of metals and alloys by X-ray powder diffraction methods*. University College Cardiff Press.
- NOWACKI J. 2008. *Stal dupleks i jej spawalność*. Przegląd Spawalnictwa, 10: 34–45.
- SENCZYK D. 1996. *Dyfraktometria rentgenowska w badaniach stanów naprężenia i własności sprząstych materiałów polikrystalicznych*. Wydawnictwo Politechniki Poznańskiej.